Development of Grinding Simulation based on Grinding Process

T. ONOZAKI A. SAITO

This paper describes grinding simulation technology to establish the generating mechanism of chatter and grinding burn. This technology consists of two modules based on grinding processes. The chatter prediction module can accurately predict chatter by analyzing the grinding force from the interference area of the wheel and workpiece. The grinding burn prediction module can predict grinding burn by calculating the distribution factor of grinding heat in detail. The validity of both modules is verified by comparing the predicted results to the experimental ones.

***Key Words**: grinding simulation, chatter, grinding burn, grinding force, distribution factor of grinding heat*

1. Introduction

For a company such as JTEKT, which not only produces grinding machines for automobile parts, but also heavily uses grinding processes in its production of automotive parts and other parts, it is important to prevent quality problems in grinding to realize high quality, on-time delivery and low cost. As quality problems in grinding, chatter (vibration between wheel and workpiece during grinding cycle) and grinding burn (change of metallographic structure caused by grinding heat), occurs frequently. From this viewpoint, first of all, it is necessary to reveal the generating mechanism of these quality problems, followed by development of the grinding simulation technology which predicts chatter and grinding burn based on the machining process of grinding.

There have been some researches concerning prediction of chatter, for example, where chatter is predicted by using estimated grinding force from cutting depth of the abrasive grains[1)~3)]. There have also been researches concerning prediction of grinding burn, which focuses on the distribution of grinding heat into the workpiece to determine the workpiece temperature closely related to grinding burn[4)~7)], and which experimentally studied about the cooling effects of the coolant on grinding burn[8)~10)]. On this research, an accurate prediction of chatter and grinding burn, referring to the previous researches, has been thought as a method to study them in detail. There are two important points to achieve this. One is to predict chatter by analyzing the grinding force from the precise interference area of the wheel and the workpiece. The other is to predict grinding burn by calculating

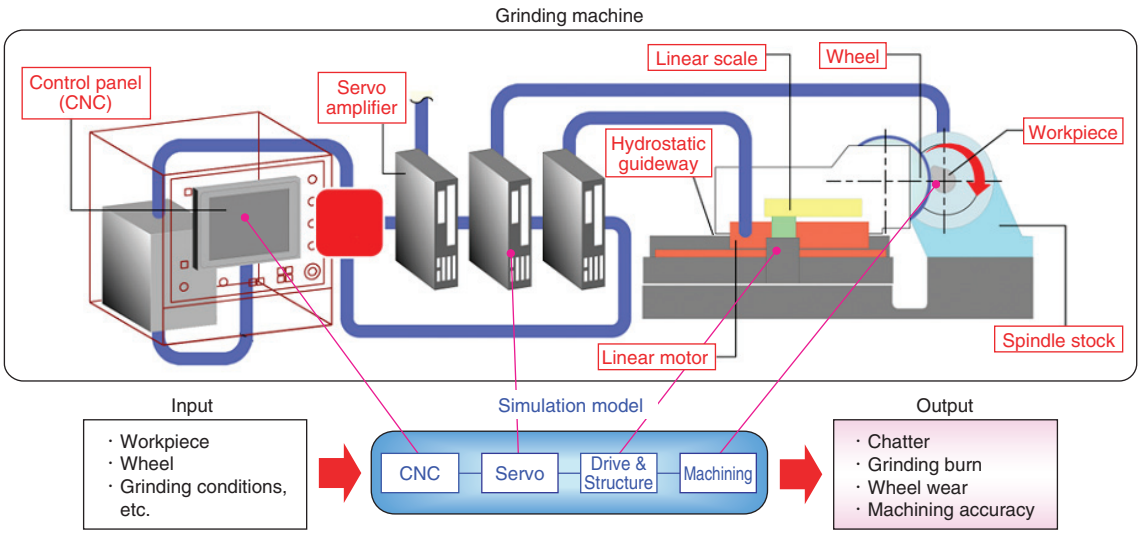

Fig. 1 Schematic view of total simulator for grinding machine

the distribution factor of grinding heat in detail, with consideration of cooling effects of coolant.

To predict machining accuracy of a workpiece, JTEKT has been working to establish models of the four core elements (CNC, servo, drive & structure, and machining) of a grinding machine and has developed a total simulator for grinding machine by linking them as shown in **Fig. 1**. The grinding simulation technology described in this paper uses precise machining models based on grinding process, which can predict such critical process outcomes as chatter and grinding burn, to reveal their generating mechanism. This technology is consisted of the chatter prediction module and the grinding burn prediction module. They are theorized by considering the relationship between the grinding force and the interference area of the wheel and the workpiece, and by considering the distribution factors of grinding heat in detail, respectively. The validity of both modules is verified by comparing the predicted results to the experimental ones.

2. Machining Process of Grinding

2. 1 Machining Model

The machining process of grinding is illustrated in **Fig. 2**. The four elements which constitute the machining process are wheel as an assemblage of abrasive grains, workpiece, chip and coolant.

To begin with, grinding is considered from the microscopic viewpoint. It is seen that single grain cutting takes place due to interference between the abrasive grain and the workpiece, which results in force and heat generation. Then, grinding is considered from the macroscopic viewpoint, as an assemblage of the single grain cutting. From this, the interference between the wheel and the workpiece brings about grinding force and grinding heat generation, which are predicted to cause chatter and grinding burn. In addition to this, the states of the abrasive grains and the wheel are also considered to change throughout the machining process of grinding. Taking such machining process into account, a machining model of grinding is formulated from the viewpoint of chatter and grinding burn as shown in **Fig. 3**. In the following subsections, the chatter prediction module and the grinding burn prediction module in **Fig. 3** are described in detail.

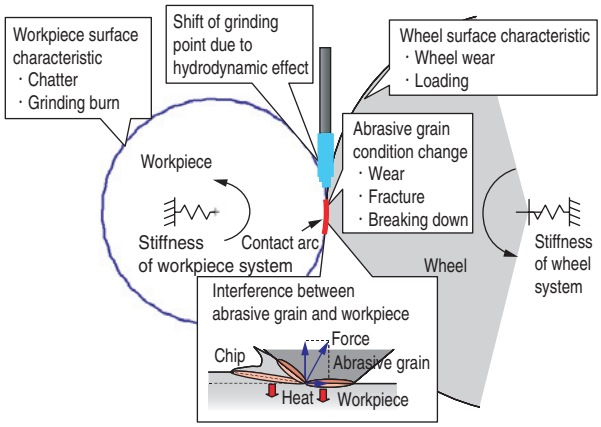

Fig. 2 Machining process of grinding

2. 2 Chatter Prediction Module

2. 2. 1 Definition of Chatter

In this paper, chatter is defined as "vibration between wheel and workpiece during grinding cycle." The vibration of this definition can be divided into forced vibration and self-excited vibration. Forced vibration depends on the disturbance displacement and grinding force. Their sources are wheel and workpiece eccentricity, wheel unbalance and the natural frequencies of the machine. Self-excited vibration mainly depends on regenerative effect. Its source is the instability of the grinding system. Instability depends on the waviness of the wheel, caused by non-uniform wear and loading of the wheel, and depends on the waviness of the workpiece caused by the interference between the wheel and the workpiece.

2. 2. 2 Focal Point

In the study of chatter, it is important to consider the fluctuation of grinding force due to the chronological change of interference between the wheel and the workpiece. By considering the relation between the fluctuation of the grinding forces and stiffness of wheel and workpiece systems, it is possible to study forced vibration due to the natural vibration of the machine, etc. as well as the self-excited vibration due to instability of the system.

Taking this point into consideration, we have focused on the chronological change of interference area between the wheel and the workpiece. In addition, a geometrical calculation procedure to determine the chronological

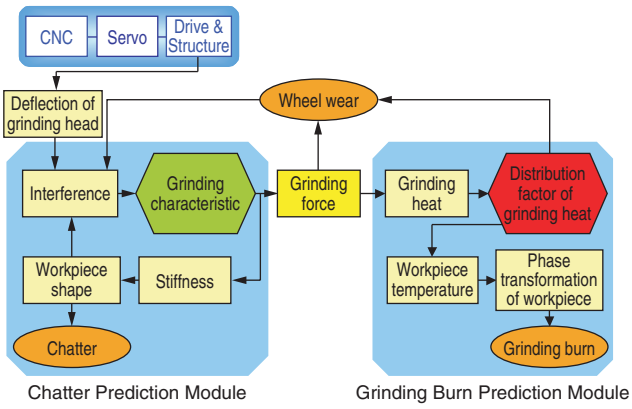

Fig. 3 Machining model of grinding

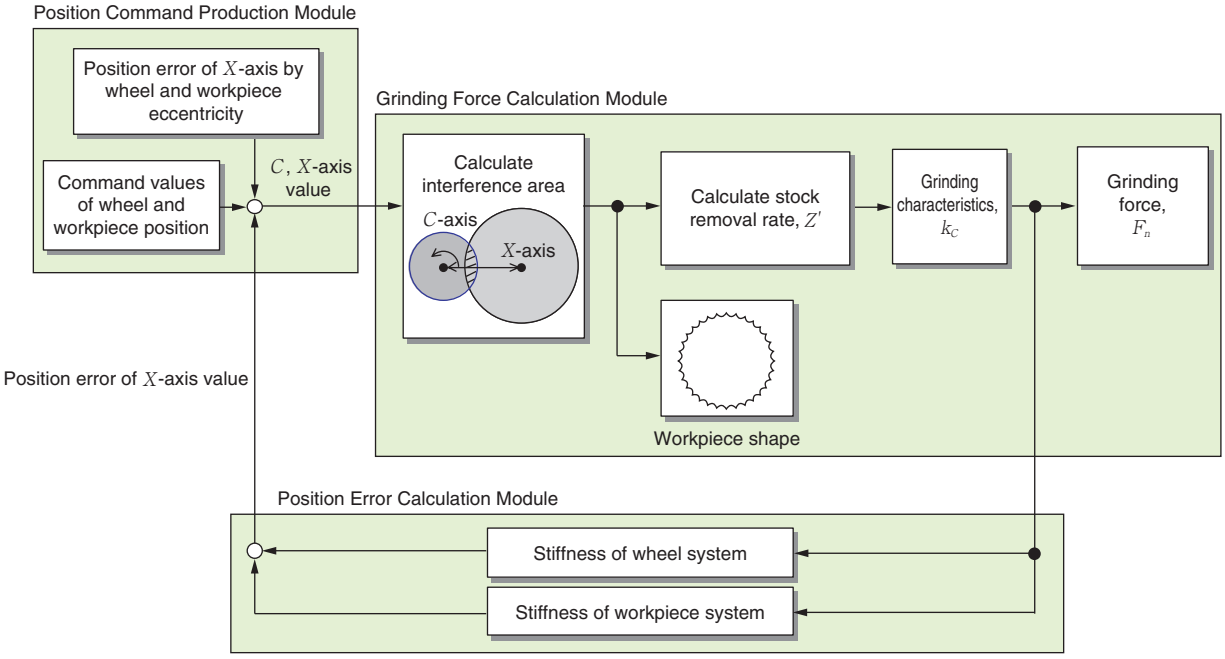

Fig. 4 Procedure for predicting chatter

change of interference area is worked out taking into account the geometry of wheel and the workpiece successively.

2. 2. 3 Chatter Prediction Procedure

The procedure for predicting chatter is shown in **Fig. 4**, which is built on the preceding conceptual framework. Here, the procedures are grouped into three modules according to their functions. The functions of each module and specific computation method for chatter prediction are described below. Although these procedures are applicable to any grinding type, here a cylindrical plunge grinding, which is the most basic, is taken as an example.

① Position Command Production Module

From the position command values for the wheel and workpiece, the rotation angle of the workpiece (called the C-axis value) and the distance between the wheel and the workpiece centers (called the X-axis value) at time t are calculated. Considering that the X-axis value is subjected to cyclic vibration due to eccentricity of the wheel and/or the workpiece or other reason, the C-axis and X-axis values can be expressed as follows:

$$\begin{cases} C = \omega t \\ X = X_0 - \dfrac{v_X t}{2} + \sum_{i=1}^{N} A_i \sin(2\pi f_i t) \end{cases} \quad (1)$$

where, ω: angular velocity of the workpiece, X_0: X-axis value at the start of process, v_X: infeed rate of the wheel, A_i: half amplitude of vibration due to eccentricity, etc, N: the maximum order to be considered, f_i: ith frequency of vibration.

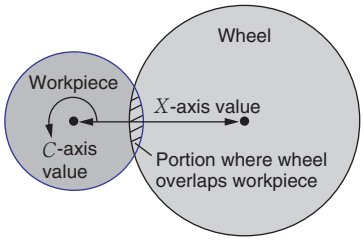

Fig. 5 General geometric relationship between wheel and workpiece

② Grinding Force Calculation Module

Considering the C-axis and X-axis values calculated in Position Command Production Module (①), a general geometric relationship between the wheel and the workpiece is as shown in **Fig. 5**. As noted in this figure, the portion where the wheel overlaps the workpiece is the interference area. After the geometrical calculation of this area, the interference per unit time Z' (called stock removal rate) is obtained. From the relationship between the calculated stock removal rate and the grinding characteristics, the grinding force is expressed as follows:

$$F_n = k_C Z' \quad (2)$$

where, F_n: normal grinding force, and k_C: gradient of normal grinding force against stock removal rate.

For information, k_C represents the grinding characteristics.

③ Position Error Calculation Module

The position error of the X-axis (difference between the position command value and the actual position) is calculated taking account of the normal grinding force

obtained in Grinding Force Calculation Module (②), and the stiffness of the wheel and workpiece systems. Then, the position error of X-axis is added to the X-axis value at the time $t + \Delta t$, and this value is given to the grinding force calculation module. Here, Δt stands for the calculation interval.

By repeating modules ① through ③ until the end of the grinding process, it is possible to predict characteristic shapes of the workpiece such as chatter.

2. 3 Grinding Burn Prediction Module

2. 3. 1 Definition of Grinding Burn

In this paper, grinding burn is defined as "the change of metallographic structure caused by grinding heat." Typical examples of this phenomenon are the re-quenched and tempered layers generated on the workpiece surface due to grinding heat when hardened steel is ground. When an untreated material is ground, a hardened layer may be generated. This is also counted as grinding burn.

2. 3. 2 Focal Point

As long as the generation of grinding burn is concerned, it is important to predict the workpiece temperature which is considered to be the main factor causing grinding burn. Also, in order to establish a theoretical basis for workpiece temperature, first of all it is necessary to set the distribution factor of grinding heat. In view of this, the distribution factor of grinding heat was selected as the focal point.

2. 3. 3 Theory for Prediction of Workpiece Temperature

To begin with, in order to study the distribution factor of grinding heat, a transfer model of the grinding heat was considered as shown in **Fig. 6**. The grinding heat generated by interference between the wheel and the workpiece is distributed in the contact arc to the wheel, the workpiece, the chip and the coolant. With the grinding heat distributed to the workpiece being transmitted to the inside of the workpiece, the workpiece temperature is increased. It is also necessary to take into consideration that the heat is carried away from the workpiece surface by the cooling effect of the coolant.

① Distribution Factor of Grinding Heat

When the grinding is viewed microscopically (i.e. at grinding point) as shown in **Fig. 7**, the grinding heat is considered to be generated by the plastic deformation in the shear plane, friction between the abrasive grain and the chip on the rake face and by friction between the wear flat of abrasive grain and the workpiece. In particular, the distribution factor of the grinding heat assigned to the workpiece can be determined by considering the heat transfer on the shear plane and the wear flat of the abrasive grain. Using Jaeger's theory[11] for moving heat source, the heat distribution factor to the workpiece on the shear plane R_{w1} can be expressed as follows:

$$R_{w1} = \frac{1}{1 + 0.752\sqrt{\dfrac{g_m(V+v)f_1(\alpha, \phi)}{K_w}}} \quad (3)$$

where, K_w: thermal diffusivity of the workpiece, and $f_1(\alpha, \phi)$: function defined by α, ϕ.

The heat distribution factor to the workpiece on the wear flat of the abrasive grain R_{w2} is expressed as follows[4]:

$$R_{w2} = \frac{1}{1 + 1.590\dfrac{k_g}{k_w\sqrt{\dfrac{(V+v)l_g}{K_w}}}} \quad (4)$$

where, k_w: thermal conductivity of the workpiece, k_g: thermal conductivity of the abrasive grain.

② Workpiece temperature

As a theoretical framework for workpiece temperature, it is assumed that the high temperature of microscopic abrasive grain at the grinding point is instantaneously transmitted to the surrounding area to form macroscopic

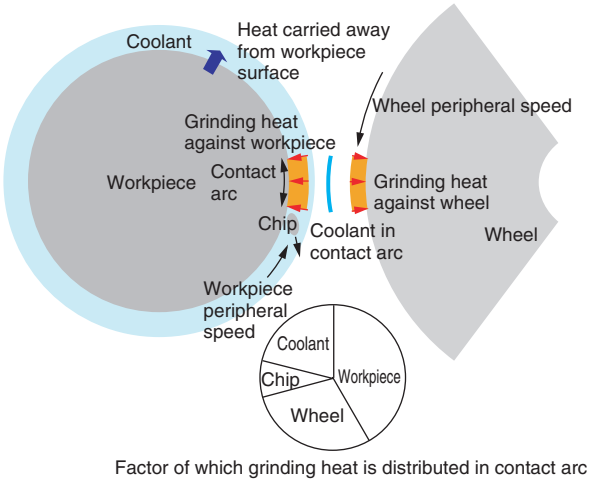

Fig. 6 Transfer model of grinding heat

α: Rake angle of abrasive grain, ϕ: Shear angle, g_m: Grain depth of cut, l_g: Length of wear flat, V: Wheel peripheral speed, v: Workpiece peripheral speed

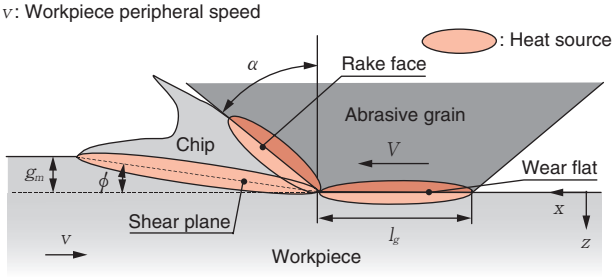

Fig. 7 Machining model with single grain at grinding point

temperature distribution. Temperature distribution in the contact arc is explored based on this assumption. Taking account of the above mentioned distribution factors of grinding heat to the workpiece, and using the theory of moving heat source taking account of cooling by the coolant, the temperature $\theta_w(X, Z)$ of the workpiece at a position (X, Z) can be expressed as follows[12].

$$\theta_w(X,\ Z) = \frac{2q_wK_w}{\pi k_w v}\left\{\int_{X-L}^{X+L} e^{-u}\mathrm{K}_0\left[\sqrt{Z^2+u^2}\right]du - \pi He^{HZ}\int_0^{\infty}\tau e^{H^2\tau^2}\mathrm{erfc}\left[\frac{Z}{2\tau}+H\tau\right]\left[\mathrm{erf}\left[\frac{X+L}{2\tau}+\tau\right] - \mathrm{erf}\left[\frac{X-L}{2\tau}+\tau\right]\right]d\tau\right\} + \theta_{w0}(X,\ Z) \quad (5)$$

$$q_w = \frac{R_wF_t(V+v)}{l_cb} \quad (6)$$

where, K_0: modified Bessel function of second kind, order zero, erf: error function, erfc: complement of error function, $\theta_{w0}(X, Z)$: initial workpiece temperature, q_w: thermal flux against the workpiece, F_t: tangential grinding force, l_c: contact arc length, and b: width of the workpiece.

Also, X, Z, L and H are dimensionless values expressed as follows:

$$X = \frac{vx}{2K_w},\ Z = \frac{vz}{2K_w},\ L = \frac{vl_c}{4K_w},\ H = \frac{2K_wh}{k_wv} \quad (7)$$

where, h: convective heat transfer coefficient of coolant.

Also, the grinding heat distribution factor to the workpiece R_w is expressed as follows:

$$R_w = \frac{R_{w1}f_2(F_{t,c}, F_{n,c}, \alpha, \phi) + R_{w2}F_{t,sl}}{F_t} \quad (8)$$

where, $F_{n,c}$, $F_{t,c}$: normal and tangential force to form chip, $f_2(F_{t,c}, F_{n,c}, \alpha, \phi)$: function defined by $F_{t,c}$, $F_{n,c}$, α, ϕ, and $F_{t,sl}$: tangential force on the wear flat of abrasive grain.

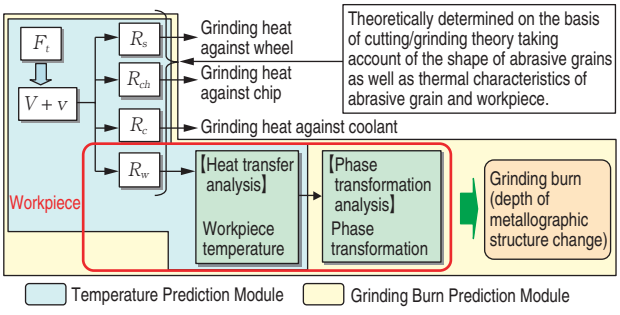

Fig. 8 Procedure for predicting grinding burn

2. 3. 4 Grinding Burn Prediction Procedure

The procedure for predicting grinding burn is shown in **Fig. 8**, which takes account of the state of the workpiece as shown in **Fig. 6** as well as the prediction theory of the workpiece temperature. Here, the detailed procedures are grouped into two modules in accordance with their functions. The functions of each module and a specific computation method for grinding burn prediction are described below.

① Temperature Prediction Module

First of all, the grinding heat is calculated by multiplying F_t and $(V + v)$. Next, the grinding heat distribution factor to the workpiece R_w is calculated by equation (8). Then, as a further heat transfer analysis, the workpiece temperature distribution $\theta_w(X, Z)$ is obtained by equation (5). Using the predicted results of workpiece temperature, the maximum temperature $\theta_{w,\,max}(Z)$ at depth Z from the workpiece surface is calculated.

② Grinding Burn Prediction Module

From the relationship between the depth Z and the maximum temperature calculated by Temperature Prediction Module (①), the value Z that satisfies the following condition is obtained and thereby the depth of grinding burn is calculated.

Depth of Hardening, Rehardening: Z_1

Z_1: The maximum of Z that satisfies $\theta_{w,\,max}(Z) > \theta_1$

Depth of Tempering: Z_2

Z_2: The maximum of Z that satisfies $\theta_{w,\,max}(Z) > \theta_2$

θ_1, θ_2: temperature determined by the metal microstructural properties of the workpiece

When further detailed information such as the volumetric ratio of each metallographic structure phase is desired in terms of the depth, a detailed phase transformation analysis would be required.

3. Results & Discussion

In this section, the results of the study on the validity of chatter prediction module and grinding burn prediction module are described.

3. 1 Result of Chatter Prediction

In order to verify validity of the chatter prediction module, results of prediction and experiment in chatter are compared. The grinding conditions for verification are shown in **Table 1**.

First of all, comparison results between predicted and experimental value of the residual cutting depth (difference between workpiece actual and target diameters) are shown in **Fig. 9**. The predicted value is very close to experimental one. This indicates that the module can accurately predict the history of workpiece shape. Then, the comparison results between predicted and experimental value of frequency analysis of

workpiece shape after grinding is shown in **Fig. 10**. The tendency of chatter generated on the workpiece in prediction is close to that in experiment. Also, the predicted out-of-roundness value is 0.40μm having good agreement with the experimental value of 0.54μm. This indicates that predicting accuracy for out-of-roundness is high as well. From these results, the validity of the chatter prediction module has been verified.

Table 1 Grinding conditions in predicting chatter

Grinding type	Single speed cylindrical plunge grinding	
Stock removal rate, $mm^3/(mm \cdot s)$	1	
Wheel	Specifications	CBN grinding wheel #120, concentration 200
	Diameter, mm	160
	Peripheral speed, m/s	119
Workpiece	Type	SCr420 carburized steel HRC64
	Diameter, mm	32
	Peripheral speed, m/s	0.50
	In-feed, mm	ϕ0.3
Coolant	Specifications	Emulsion type water soluble coolant
	Flow rate, L/min	30

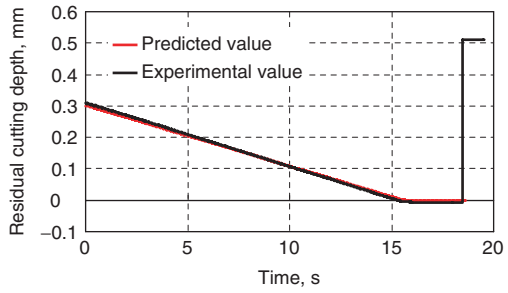

Fig. 9 Comparison results between predicted and experimental values of residual cutting depth

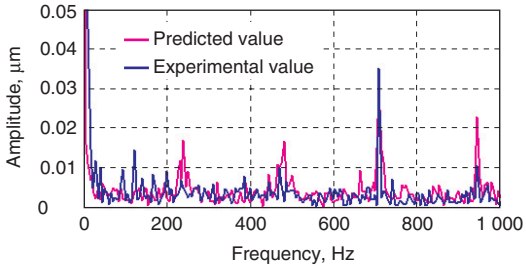

Fig. 10 Comparison results between predicted and experimental values of workpiece shape frequency analysis

3. 2 Result of Grinding Burn Prediction

In order to verify the validity of the grinding burn prediction module, results of prediction and experiment in grinding burn are compared. The grinding conditions for the verifications are as shown in **Table 2**. The parameters required in the analysis, such as the rake angle of the abrasive grain, length of the wear flat and shear angle, were estimated from observation of the wheel surface.

To begin with, comparison of prediction and experiment results concerning generation of re-quenching is summarized in **Table 3**. The prediction results agree qualitatively well with those of experiments. Then, prediction results of the maximum temperature at a different depth from the workpiece surface are shown in **Fig. 11**. The graph suggests that, in the case when

Table 2 Grinding conditions in predicting grinding burn

Grinding type	Single speed cylindrical plunge grinding	
Stock removal rate, $mm^3/(mm \cdot s)$	5, 12, 20	
Wheel	Specifications	CBN grinding wheel #120, concentration 200
	Diameter, mm	400
	Peripheral speed, m/s	120
Workpiece	Type	SCM415H carburized steel HRC60
	Diameter, mm	68
	Peripheral speed, m/s	0.53, 1.77
Coolant	Specifications	Emulsion type water soluble coolant
	Flow rate, L/min	30

Table 3 Comparison results between prediction and experiment in re-quenching

Workpiece peripheral speed, m/s	0.53			1.77		
Stock removal rate, $mm^3/(mm \cdot s)$	5	12	20	5	12	20
Prediction	No	No	Yes	No	No	Yes (minimal)
Experiment	No	No	Yes	No	No	No

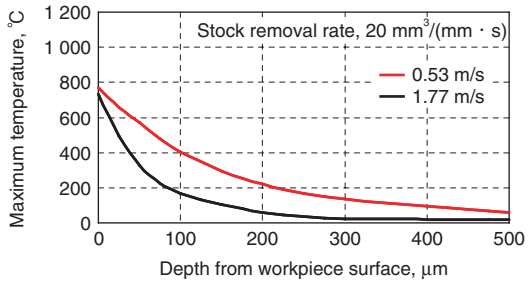

Fig. 11 Prediction results of maximum temperature of workpiece

workpiece peripheral speed is faster, the maximum temperature at each depth is suppressed, and hence the possibility of generating grinding burn is reduced. This prediction result is qualitatively consistent with the generally accepted knowledge, "In the case when the volume of material removed and the grinding time are the same, grinding conditions with faster workpiece peripheral speed and thinner depth of cut is advantageous to suppress the grinding burn." From these results, the validity of the grinding burn prediction module has been verified qualitatively. In the future, a quantitative evaluation is planned.

4. Conclusion

To develop grinding simulation technology based on the grinding process, the chatter prediction module and the grinding burn prediction module have been constructed. The validity of both modules has been verified by comparing the predicted results to the experimental ones. From this, the modules have been confirmed that they could identify qualitative tendency in terms of chatter and grinding burn. From these results, this technology was known to be effective to reveal the generating mechanism of chatter and grinding burn.

In the future, we will improve the analysis accuracy of both modules aimed at quantitative prediction of chatter and grinding burn. Also, we will try to utilize the developed grinding simulation technology in-house facilities for the optimization of grinding conditions, the improvement of efficiency in selecting grinding conditions and for the development of grinding machines.

References

1) T. Hoshi: Seimitsukikai, **49**, 12 (1983) 1680.
2) M. Miyashita: Kakougijyutsu Data File, **5**, 7.
3) I. Inasaki: Annals of the CIRP, **50**, 2 (2001) 515.
4) K. Takazawa: Seimitsukikai, **30**, 12 (1964) 914.
5) S. Malkin: ASME J. Engineering for Industry, **96**, 4 (1974) 1177.
6) S. Malkin: ASME J. Engineering for Industry, **96**, 4 (1974) 1184.
7) S. Malkin: Annals of the CIRP, **27**, 1 (1978) 233.
8) H. Yasui: Seimitsukikai, **48**, 5 (1982) 609.
9) H. Yasui: Seimitsukougakkaishi, **56**, 3 (1990) 521.
10) H. Yasui: Seimitsukougakkaishi, **56**, 11 (1990) 2087.
11) J. C. Jaeger: Proceedings of Royal Society of New South Wales, **76** (1942) 203.
12) N. R. DesRuisseaux, R. D. Zerkle: ASME J. Heat Transfer, **92**, 3 (1970) 456.

T. ONOZAKI* A. SAITO**

* *Mechatronic Systems R&D Department, Research & Development Center, Dr. Eng.*
** *Mechatronic Systems R&D Department, Research & Development Center*